JOURNAL OF PLANKTON RESEARCH | VOLUME 23 | NUMBER 12 | PAGES 1345–1360 | 2001

Trophic control of biogenic carbon export in Bransfield and Gerlache Straits, Antarctica

PABLO SERRET[1,4], EMILIO FERNÁNDEZ[2], RICARDO ANADÓN[1] AND MANUEL VARELA[3]

[1]UNIVERSIDAD DE OVIEDO, DEPARTAMENTO DE BIOLOGÍA DE ORGANISMOS Y SISTEMAS, C/ CATEDRÁTICO R URÍA, S/N, E33071, OVIEDO, SPAIN, [2]UNIVERSIDAD DE VIGO, DEPARTAMENTO DE ECOLOGÍA Y BIOLOGÍA ANIMAL, FACULTAD DE CIENCIAS, CAMPUS LAGOAS-MARCOSENDE, E36200 VIGO, SPAIN, [3]INSTITUTO ESPAÑOL DE OCEANOGRAFIA, MUELLE DE ÁNIMAS S/N. APDO. 130, E15080, LA CORUÑA, SPAIN

[4]PRESENT ADDRESS: UNIVERSIDAD DE VIGO, DEPARTAMENTO DE ECOLOGÍA Y BIOLOGÍA ANIMAL, CAMPUS LAGOAS-MARCOSENDE, E36200 VIGO, SPAIN

CORRESPONDING AUTHOR: P. SERRET. E-MAIL: pserret@uvigo.es

Size-fractionated chlorophyll a and photosynthetic carbon incorporation, microbial oxygen production and respiration and particulate vertical flux were measured in January 1996 at three regions, characterized by distinct hydrographic fields and planktonic communities, of the Antarctic Peninsula: (1) a diatom-Phaeocystis sp., dominated community associated with the relatively stratified waters of the Gerlache Strait, (2) a nanoplankton-Cryptomonas sp. dominated assemblage at the Gerlache–Bransfield confluence; and (3) a nano- and picoplankton community in mixed waters of the Bransfield Strait. Despite the marked differences in both community structure and total phytoplankton biomass and primary production, and against predictions from models about trophic control of C export, the lowest respiration rates were measured at Bransfield (pico- and nanoplankton), and no difference was observed between the Gerlache (large diatoms) and Bransfield stations in relative vertical particle flux (6.4 vs. 5.1 % of suspended C; 14.9 vs. 10.4 % of net community production, respectively). Growth and loss rates of the phytoplankton population studied for each community indicate that microbial populations can be explained by in situ growth, but spatial (diatom-Phaeocystis sp., bloom) and temporal (diatom-Phaeocystis sp. bloom and nanoplankton communities) scales of study were shown to be insufficient for addressing the coupling between primary production and biogenic carbon export, especially after the appreciation of the accumulation of dissolved organic carbon in the water column. This would explain the unexpected results and highlights the necessity of including the mechanisms controlling accumulation and consumption of dissolved organic matter into conceptual models about the trophic control of C export.

INTRODUCTION

Most conceptual models on the control of biogenic carbon export from the euphotic layer highlight the importance of plankton trophic dynamics [e.g. (Legendre and Rassoulzadegan, 1996; Boyd and Newton, 1999)]. According to these models, phytoplankton cell size integrates the structure of trophic webs, because the factors regulating relative growth and loss rates of the different populations, i.e. competitive advantage of small algae for nutrients and light uptake, inverse relationship between cell size and sinking rate, greater susceptibility of picoplankton to grazing control, are all dependent on cell size (Legendre and Le Fèvre, 1989; Riegman *et al.*, 1993; Kiørboe, 1993). Legendre and Rassoulzadegan (Legendre and Rassoulzadegan, 1996) concluded that the characteristics of trophic webs that determine the fate of biogenic carbon (remineralization within the euphotic layer, transfer to trophic webs, or export to deep layers) can be summarized into two key factors: size spectrum of primary producers and the degree of coupling between the processes of production and consumption of organic matter. In systems dominated by microbial food webs most of the fixed energy is expected to be consumed within the euphotic layer, while in those dominated by herbivore or multivore webs [*sensu* (Legendre and Rassoulzadegan, 1995)], higher export of carbon from the euphotic zone occurs

as a consequence of direct sedimentation of phytoplankton cells or zooplankton faecal pellets.

The phytoplankton size spectrum is relatively easy to estimate at a basic level, either as biomass or activity, by means of size fractionation of chlorophyll *a* concentration or photosynthetic C incorporation. The opposite is true for the coupling between the processes of production and consumption of organic matter. A frequently used approach consisted of the independent estimation of auto- and heterotrophic biomasses and activities, together with direct measurements of sedimentation rates (Lignell *et al.*, 1993; Biscaye *et al.*, 1994; Rivkin *et al.*, 1996). This approach necessitates the assumption of several hypotheses about pathways of organic matter circulation in planktonic communities, and implies the use of diverse methodologies for the measurement of the different variables, as well as the final conversion of the various results to common units (usually carbon). This brings together important uncertainties in the final balance between production and consumption of organic matter.

An alternative approach is the direct estimation of microbial net community production, i.e. the difference of phytoplankton gross production minus total microbial respiration, from measurements of *in vitro* changes in seawater oxygen concentration. Oxygen net production summarizes the microbial trophic dynamics, being independent of the community structure, and provides a direct estimate of one of the two key characteristics of plankton communities proposed by Legendre and Rassoulzadegan as controlling factors of the fate of biogenic carbon in the ocean: the degree of coupling between the processes of production and consumption (Legendre and Rassoulzadegan, 1996).

The ultimate aim of this work was the empirical verification of conceptual models about trophic control of organic carbon export, which predict that a direct relationship exists between the potential for C export from the productive zone of the pelagic ecosystem and the organization of pelagic trophic webs. With this aim, sampling was carried out to study the relationship between phytoplankton size (a variable summarizing community structure), production/respiration balance (a variable summarizing community processes) and particulate carbon export. That is, a study on the modulation of the relationship between organic matter production and carbon export by the structure and functioning of trophic webs. This study was conducted during January 1996 in coastal waters of the Antarctic Ocean, where elevated spring primary production rates and the existence of a rapid succession from a community dominated by large diatoms to a nanophytoplankton-dominated community are well documented (Holm-Hansen and Mitchell, 1991; Moline and Prezélin, 1996). Such a succession has been observed to be accompanied by a shift from herbivore or multivore trophic webs, with elevated particulate carbon export, to a microbial food web, with increased recycling of organic matter in the upper mixed layer and, hence, lower particulate carbon export (Karl 1993).

METHOD

Sampling

A transect of 14 stations across Gerlache Strait and onto Bransfield Strait was sampled in January 1996 during FRUELA95 cruise (Figure 1). In addition to Conductivity, Temperature, Depth (CTD) casts, samples for size-fractionated chlorophyll *a* and microplankton cell counts were taken. Once this transect was sampled, four flux stations were determined to cover the observed range in physical conditions and phytoplankton communities (Figure 1). The time lag between transect and flux stations sampling ranged from 3 to 12 days. Vertical profiles of temperature and conductivity were performed with an EG&G MKIIIc CTD fitted to an EG&G 1015 rosette. Water samples for O_2 and size-fractionated chlorophyll *a* concentrations, microplankton cell counts, size-fractionated photosynthetic C incorporation and microbial O_2 production and respiration were collected from five depths with 12 litre Niskin bottles fitted to the rosette.

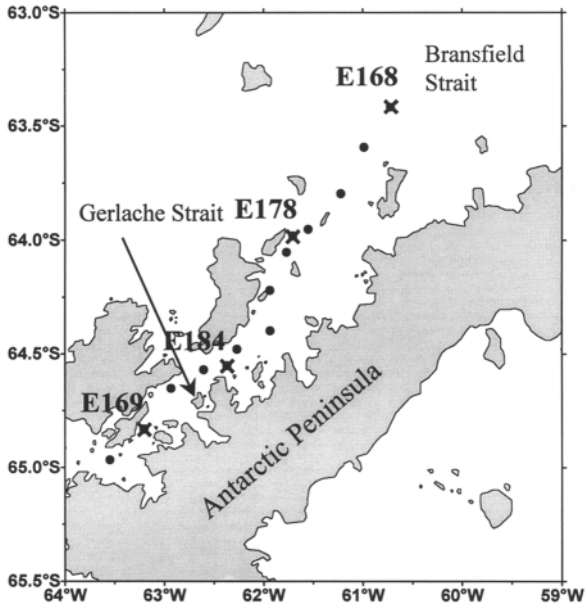

Fig. 1. Map of the study area in the western region of the Antarctic Peninsula, showing the position of stations sampled during the Gerlache-Bransfield transect (•) and flux stations (×) of FRUELA 95 cruise (January 1996).

Dissolved oxygen

A 250 ml gravimetrically calibrated, borosilicate bottle was carefully filled from every Niskin bottle by means of a silicone tube. Fixing and storage procedures, reagents and standardization followed the recommendations of Grasshoff *et al.* (Grasshoff *et al.*, 1983). Dissolved oxygen concentration was measured through automated precision Winkler titration performed with a Metrohm 716 DMS Titrino, using a potentiometric end point (Oudot *et al.*, 1988; Pomeroy *et al.*, 1994). Aliquots of fixed samples were delivered with a 50 ml overflow pipette.

Size-fractionated chlorophyll *a* concentration

Samples of sea water (250 ml) were sequentially filtered onto 10, 2 and 0.2 μm pore size Poretics polycarbonate filters, which were kept deep-frozen (–20°C). Chlorophyll *a* concentration was determined using a Turner Designs 10 fluorometer after extraction in 90% acetone for 24 h at 4°C (Strickland and Parsons, 1972).

Microplankton cell counts

Polyethylene bottles (250 ml) containing Lugol's solution were filled with sea water from the sampling depths. Enumeration of organisms was carried out with an inverted microscope on 50 ml composite sedimentation chambers.

Size-fractionated photosynthetic C incorporation

Rates of phytoplankton C incorporation in 0.2–2 μm, 2–10 μm and >10 μm phytoplankton size classes were determined following JGOFS protocols (Knap *et al.*, 1996). Three replicates of 250 ml water samples, previously inoculated with $NaH^{14}CO_3$ were incubated *in situ*. Incubations always started at dawn and lasted 24 h. Once the incubation had finished, samples were filtered under low vacuum pressure (<100 mmHg) following the same procedure as described for size-fractionated chlorophyll *a*. Filters were decontaminated by exposing them overnight to HCl fumes. Scintillation cocktail was added to the samples and the radioactivity was measured with a Packard scintillation counter. Quenching was corrected by using the internal standard method.

Microbial oxygen production and consumption

Rates of microbial community O_2 production and consumption were determined by *in vitro* changes in seawater O_2 concentration after light and dark bottle incubations. Sampling and incubation (24 h, *in situ*) were carried out at the same depths, simultaneously and under the same conditions as for C incorporation experiments. Twelve 250 ml, gravimetrically calibrated, borosilicate bottles were carefully filled from every Niskin bottle by means of a silicone tube, overflowing >500 ml. Filled bottles were immediately closed and kept, in darkness, in a deck incubator refrigerated with surface water. This procedure minimized temperature changes until the whole set of bottles was filled, and the buoy, carrying the *in situ* incubation device and a shallow sediment trap, was ready for deployment. An initial set of four dark bottles was fixed at once, the remaining (four dark and covered with aluminium foil, four light) were bonded to the buoy at the depths of origin of the water sampled. After the incubation period, dissolved oxygen concentration was determined following the method described above.

Particulate vertical flux from the euphotic zone

Shallow sediment traps similar to those developed by Knauer *et al.* and modified by Karl *et al.* were used (Knauer *et al.*, 1979; Karl *et al.*, 1991). The traps were fastened to the same buoys as incubation bottles and placed 3 m below the deepest incubation tray (50–64 m), well below the euphotic (down to 1% incident irradiance) depth (20 m at E169, E184 and E178; 30 m at E168). Traps were kept in the water for 24 h (same as incubations), which provided enough material for later analyses. From each of the four tubes of the trap, subsamples were obtained for the analysis of particulate carbon and nitrogen content and chlorophyll *a* concentration. In order to estimate the viability of sedimented cells, photosynthetic C incorporation was determined by means of incubations with $NaH^{14}CO_3$ of samples from material collected by the traps.

RESULTS

Spatial variability: Gerlache-Bransfield section

Hydrographic and chemical conditions

The vertical distribution of temperature, salinity and the percentage of oxygen saturation in the upper 100 m along the Gerlache–Bransfield transect is presented in Figure 2. A marked hydrographic front was found at the northeast mouth of Gerlache Strait, near station E178. This front separated colder, saltier and vertically more homogeneous Bransfield Strait waters from waters of central Gerlache strait, showing haline stratification after freshwater inputs from glacier melting.

In the central part of Gerlache strait, where flux stations E169 and E184 were located, O_2 concentration

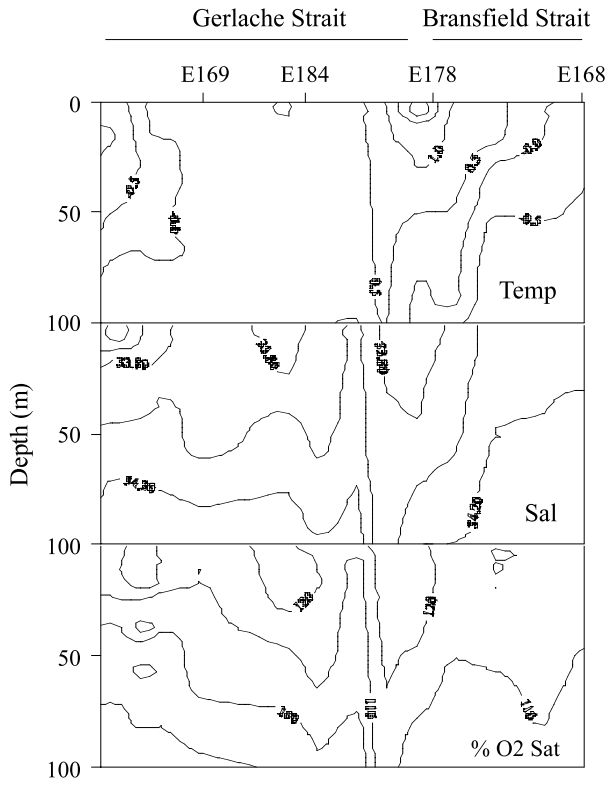

Fig. 2. Spatial distribution of temperature, salinity and the percentage of oxygen saturation across the Gerlache-Bransfield transect (January 1996).

was higher than the level of saturation in the upper 60 m; the highest values (130% of O_2 saturation) were measured in the upper 5–10 m at the region showing the highest degree of vertical stability. In Bransfield, O_2 saturation was >100% down to depths >200 m. The distribution of O_2 saturation at the Gerlache–Bransfield confluence suggested the convergence of surface water at the eastern part of the front, where values >110% were measured down to 120 m depth, and upwelling of subsurface water at the western side, where relatively low saturation levels were observed at the surface.

Although nutrient distributions were related to phytoplankton biomass and activity, concentrations in the upper mixed layer were high (>75 μmol SiO_2 kg^{-1}, >22 μmol NO_3 kg^{-1}) throughout the region of study (Castro *et al.*, 2002).

Chlorophyll a *concentration*

The spatial distribution of total and size-fractionated chlorophyll *a* concentration (Figure 3) exhibited a close relationship with the hydrographic field. A dense patch of >10 μm phytoplankton was observed in Gerlache Strait, where the highest phytoplankton biomass, at the central region, coincided with the highest water column vertical stability and O_2 saturation values. Phytoplankton in Gerlache was dominated by large chain-forming diatoms, the large flagellate *Pyramimonas* sp. and colonies of *Phaeocystis* sp. In Bransfield Strait, cells >10 μm constituted only ca. 5% of total phytoplankton biomass, while nanoplankton (cells between 2 and 10 μm size) was the most abundant fraction, especially in subsurface waters (70–80% of total phytoplankton biomass). Diatoms were very scarce, while the abundance of *Cryptomonas* sp., free *Phaeocystis* sp. cells and microflagellates was high. The front at the confluence between Gerlache and Bransfield Straits clearly separated both communities and drove the spatial distribution of phytoplankton biomass, which showed high deep values at the eastern side (convergence) and low surface values at the western part (divergence). The elevated surface phytoplankton biomass and relatively high deep biomass at the eastern part of the front consisted almost exclusively of pico- and nanoplankton (namely, *Cryptomonas* and dinoflagellates), which clearly distinguished it from the biomass found at similar depths in Gerlache.

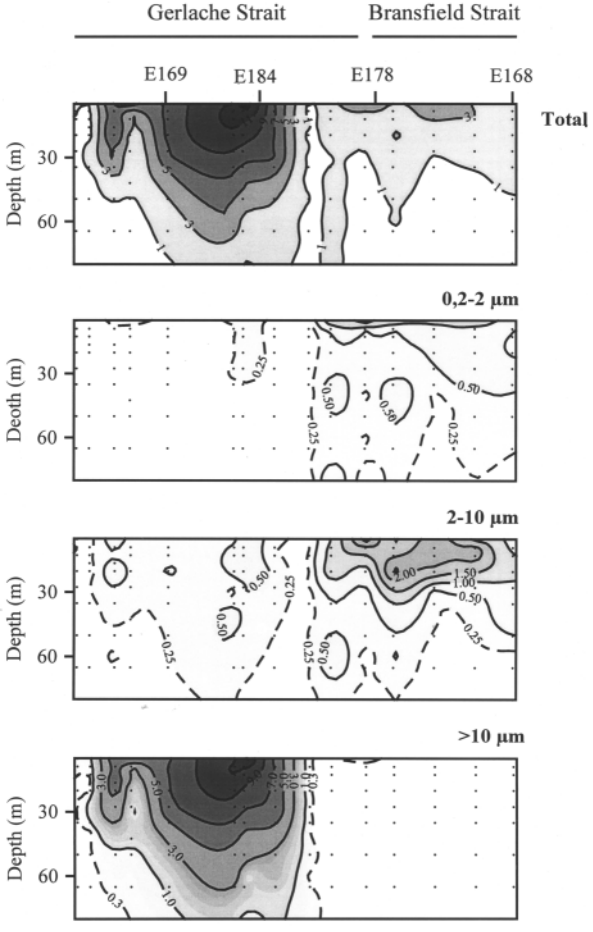

Fig. 3. Spatial distribution of total and size fractionated chlorophyll *a* concentration (mg m^{-3}) across the Gerlache–Bransfield transect (January 1996).

Carbon and oxygen fluxes

Microbial production and respiration, together with vertical particle flux were measured at four stations representative of the regions described above (positions are shown in Figures 1 to 3). Two flux stations were located in central Gerlache Strait: E184, near the zone of highest vertical stability and chlorophyll *a* concentration, and E169, in the marginal zone of the patch of high biomass of large-sized phytoplankton. Flux station E168 was placed in Bransfield Strait waters, while flux station E178 was located at the *Cryptomonas*-dominated high surface chlorophyll *a* patch at the frontal zone of the Gerlache–Bransfield confluence.

Hydrographic characteristics of the water column

The times separating sampling of the Gerlache–Bransfield transect and the visit to flux stations were 3, 5, 10 and 12 days for E168, E169, E178 and E184, respectively. Figure 4 presents vertical profiles of temperature and salinity at flux and transect stations occupying the same position. Significant changes between both samplings

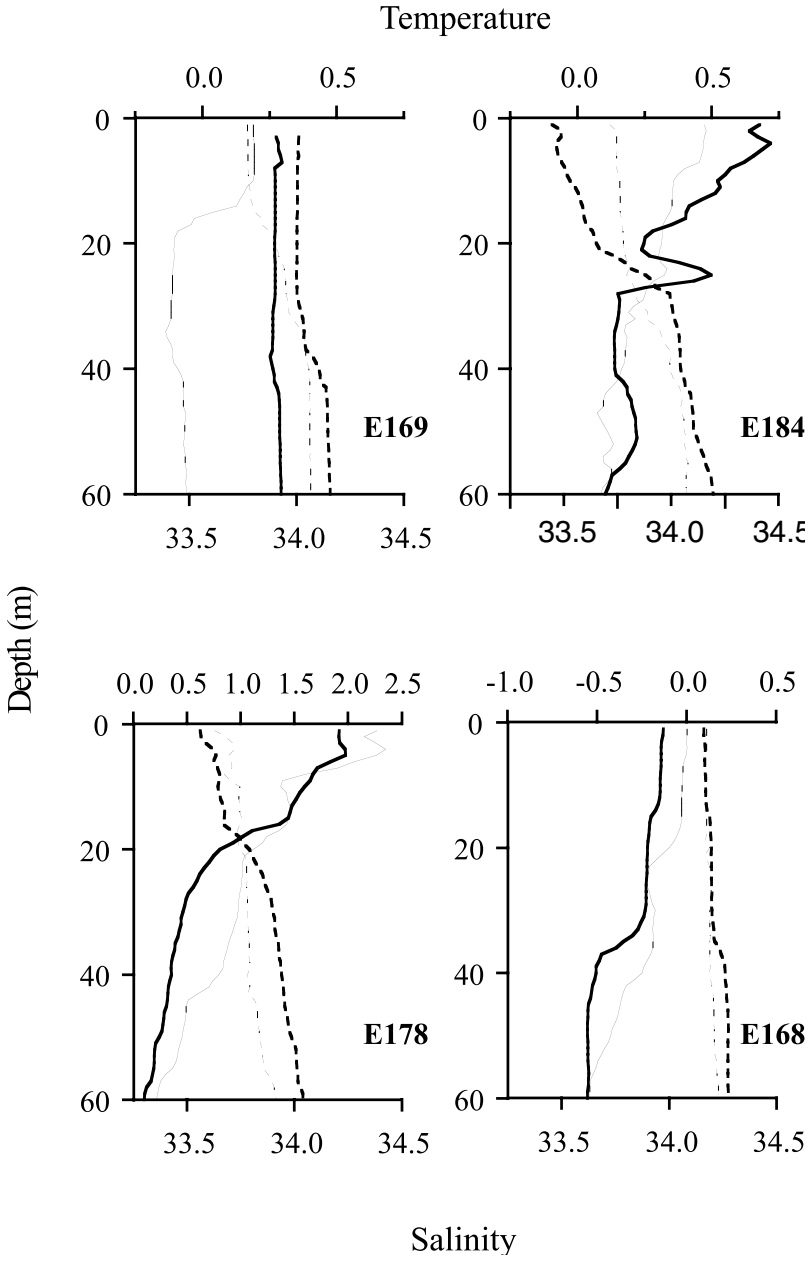

Fig. 4. Vertical distribution of temperature (solid line) and salinity (broken line) at the flux stations (thick line) and at the transect stations (thin line) occupying the same positions.

were only observed at station E169, where vertical homogeneity of the water column increased.

Chlorophyll a *concentration*

The spatial distribution of size-fractionated chlorophyll *a* remained constant during the study (Figures 3 and 5). At both Gerlache flux stations (E169 and E184), phytoplankton biomass was dominated by cells >10 μm (namely, large chain-forming diatoms, *Pyramimonas* and colonies of *Phaeocystis*). At station E169, total chlorophyll *a* concentration decreased slightly at all depths with respect to the sampling of the transect, and a surface increase of 6 mg Chl *a* m^{-3} was observed at E184 together with a subsurface decline. At station E178 total phytoplankton biomass decreased in ca. 2 mg Chl *a* m^{-3}, especially in the picoplankton fraction, although *Cryptomonas* and small dinoflagellates were still the dominant taxa. Minor changes in biomass distribution and dominant groups (*Cryptomonas*, free *Phaeocystis* cells and microflagellates) were registered at E168.

Photosynthetic carbon incorporation

Similar trends to those described for phytoplankton biomass were evident, in both total and size-fractionated C incorporation (Figure 6). The highest C incorporation rates were found at E184, where integrated primary production amounted to >3 g C m^{-2} day^{-1}. At both Gerlache stations (E169 and E184), 87% of surface and 80% of water column primary production corresponded to >10 μm phytoplankton cells. In Bransfield (E168) C incorporation by cells >10 μm was less than 10%, and total primary production was relatively high (0.8 g C m^{-2} day^{-1}) in a broad (ca. 20 m) surface layer, depicting a similar trend as chlorophyll *a* concentration. At the frontal station (E178) high rates of primary production were only measured in a thin surface layer, matching the vertical

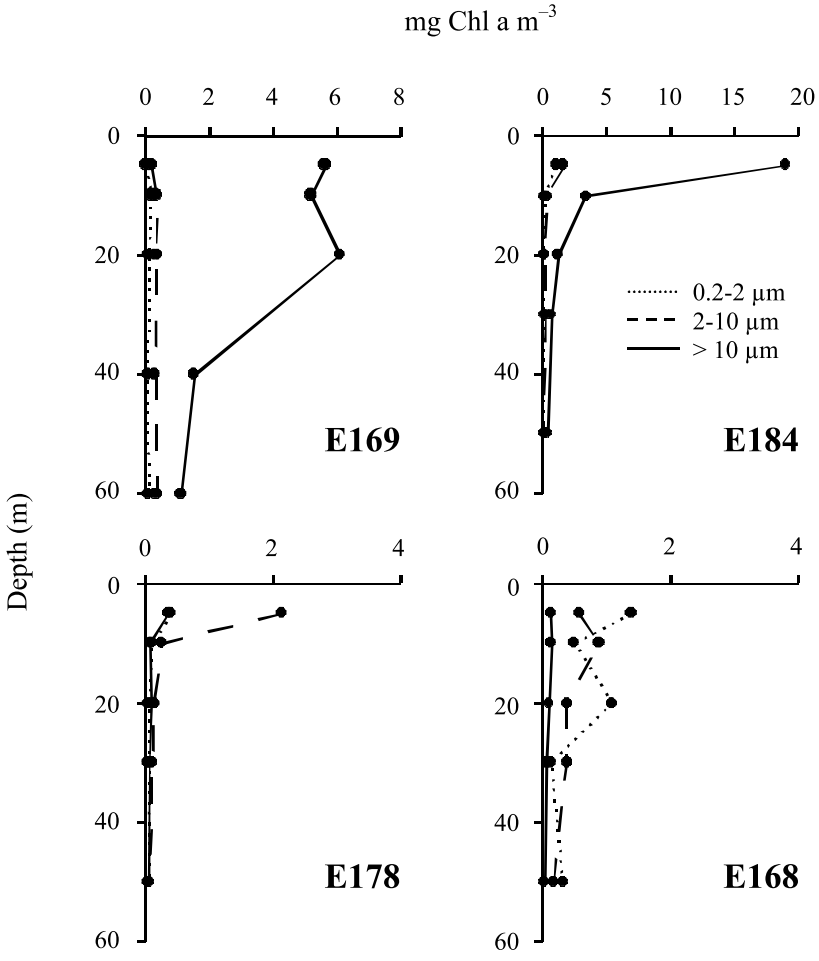

Fig. 5. Vertical distribution of size-fractionated chlorophyll *a* concentration at flux stations. Note differences in concentration scales.

pattern described for chlorophyll *a* concentration. As for phytoplankton biomass, C incorporation was also dominated by nano- and picoplankton (>90%).

Microbial oxygen production and consumption

The vertical distribution of gross O_2 production (GP) matched perfectly that of C incorporation at every sampled station (GP = 2.067 * C incorporation + 1.082; $r^2 = 0.97$; $P < 0.001$) (Figure 7). The molar ratio of O_2 GP to C incorporation was >2, clearly higher than 1.4 which is the value estimated for new production (Laws, 1991; Williams and Robertson, 1991), suggesting that C incorporation was closer to net than to gross production, as could be expected from 24 h incubation. However, as shown below, respiration rates in the dark represented a very small percentage of GP at all depths. While in Gerlache (E169 and E184) the molar ratio of net O_2 community production to C incorporation in the euphotic layer (1.46 and 1.68, respectively) was close to the theoretical value for new production, in Bransfield (E168 and E178) this ratio remained too high (2.4).

Figure 8 presents vertical profiles of O_2 gross production (GP), dark respiration (DR) and net community production (NCP) rates at every sampled station. Microbial DR rates at the nanoplankton-dominated station (E168) were almost undetectable at all depths, ca. 0.5 mmol O_2 m^{-3} day^{-1} throughout the euphotic zone, which represents 12% of GP. No appreciable changes were registered in DR rates with depth, nor in relation to phytoplankton biomass or activity. Higher DR rates were measured in Gerlache, dominated by cells >10 μm. At station E169, DR did not exhibit remarkable changes with depth, apart from a slight increase immediately below the euphotic zone (20 m depth). Positive NCP was measured in the euphotic zone, while below this layer DR exceeded GP. The highest DR rates were measured at station E184,

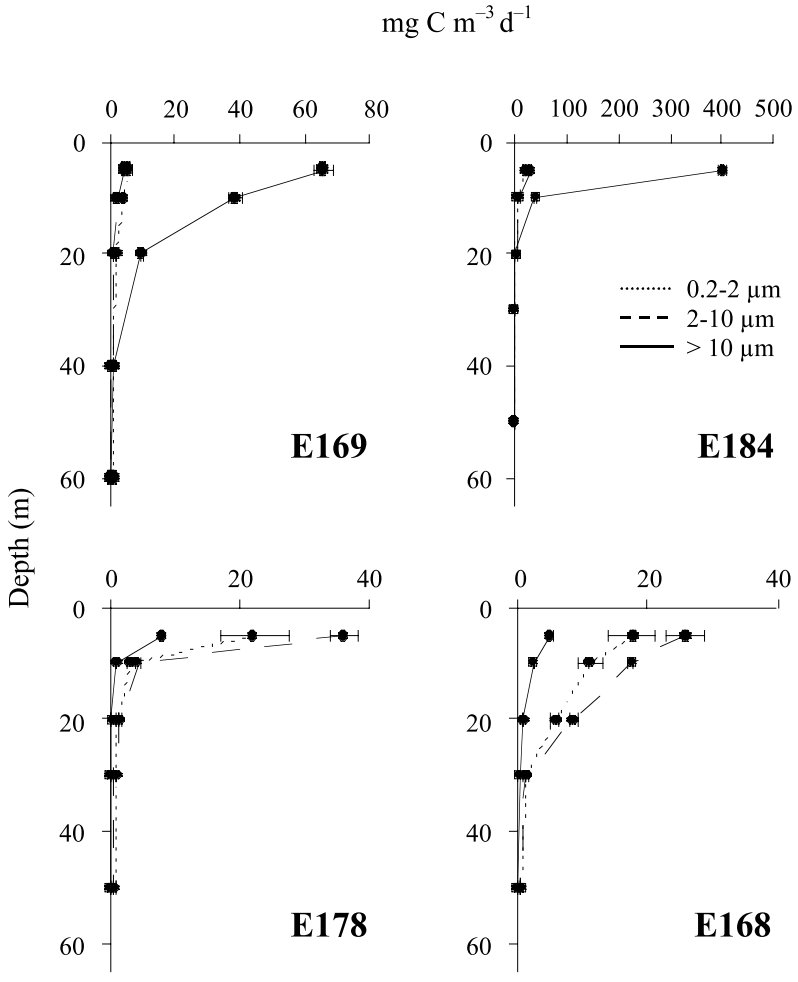

Fig. 6. Vertical distribution of size-fractionated C incorporation rates at flux stations (± SE, $n = 3$). Note differences in concentration scales.

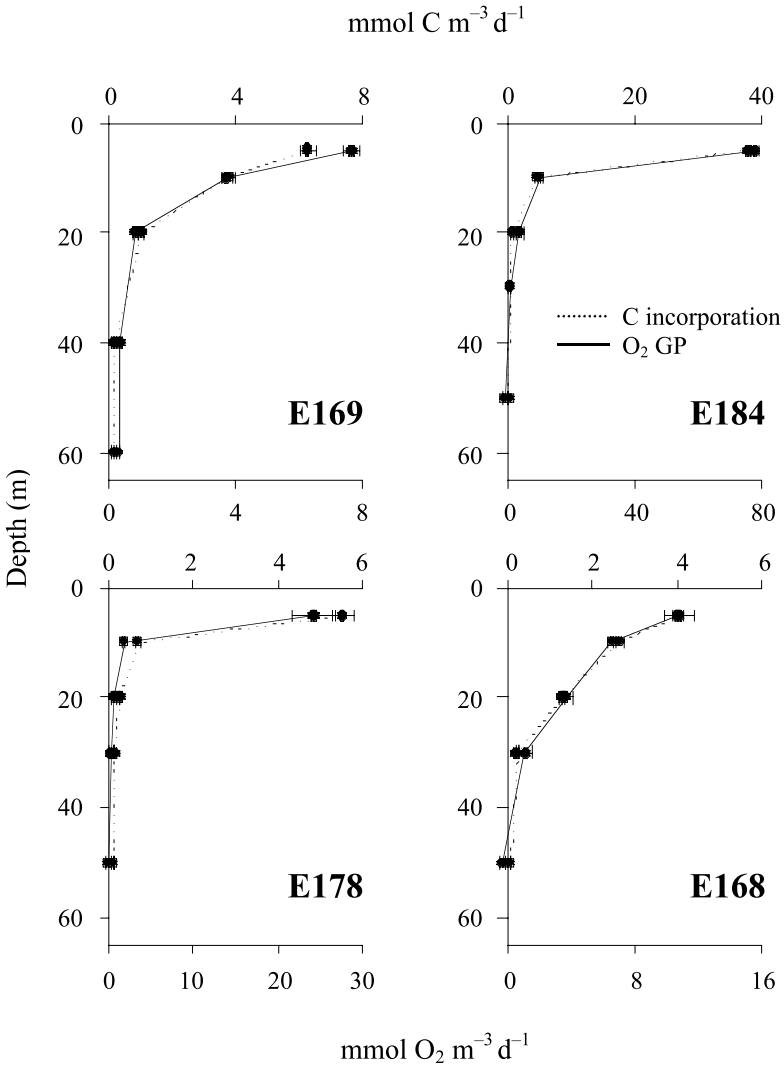

Fig. 7. Vertical distribution of total C incorporation (dashed line) and oxygen gross production (solid line) rates at flux stations. Note differences in concentration scales.

where their vertical distribution resembled that of phytoplankton biomass and production, exhibiting a surface maximum >8 mmol O_2 m^{-3} day^{-1}, and relatively high values (ca. 2.5 mmol O_2 m^{-3} day^{-1}) below 10 m depth. Positive values of NCP were found throughout the euphotic layer (20 m depth), with a surface maximum higher than 69 mmol O_2 m^{-3} day^{-1}, while negative NCP rates were measured below this layer, reaching – 4 mmol O_2 m^{-3} day^{-1} at 50 m depth. In Gerlache, higher relative aphotic respiration was found at E169 (33% of water column GP) than at E184 (15%). At the frontal station (E178), two opposite situations were found within the euphotic layer (20 m depth): very high DR and GP rates, with an elevated 'surplus' of production, at 5 m depth; and very low DR (ten times lower than at the surface) and GP rates, with NCP near zero from 10 m depth.

Particulate vertical flux from the euphotic zone

Vertical particle flux was determined at three flux stations (Table I). Data must be looked at with caution due to inherent methodological limitations of shallow sediment traps [see e.g. (Karl *et al.*, 1991; Newton *et al.*, 1994; Buesseler, 1998) and references therein]. At station E184 an elevated flux of organic matter was observed. Assuming a carbon to chlorophyll *a* ratio of 40 (Smith and Sakshaug, 1990), virtually all the organic C retained in the trap corresponded to phytoplankton-derived material. However, the photosynthetic activity of this material was very low

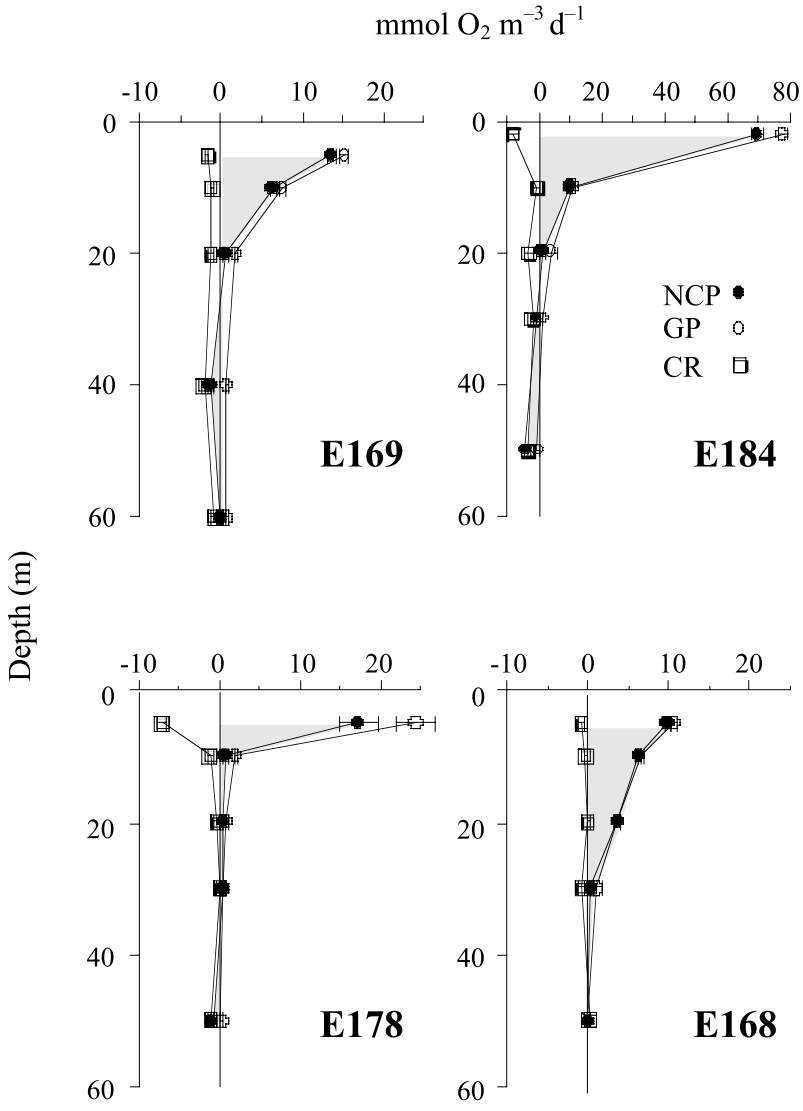

Fig. 8. Vertical distribution of gross (GP) and net (NCP) production, and dark respiration (DR) of oxygen by microplankton at flux stations (± SE, n = 4). Note differences in concentration scales.

(0.09 mg C mg Chl a^{-1} day^{-1}), which could be related to a vertical transport mediated by the abundant zooplankton faecal pellets. In Bransfield (E168), both particulate C sedimentation rate and the percentage of phytoplanktonic material were clearly lower. Finally, at station E178, a relatively high vertical flux of particulate C was measured, although the phytoplanktonic contribution was very low. Despite differences in the contribution by phytoplankton to total particle flux, at both nanoplankton-dominated stations (E168 and E178) the material collected by the traps presented a relatively high, and similar, chlorophyll *a* normalized, photosynthetic activity (1.87 and 1.57 mg C mg Chl a^{-1} day^{-1} at E168 and E178, respectively). At E168, no faecal pellets were found in the sedimented material, and at E178, their number was 2.5 times lower, in relation to total sedimented C, than in Gerlache.

Table II shows the percentage of vertical C flux with respect to phytoplankton biomass and daily production rates in the water column. The highest vertical flux percentage, both regarding suspended phytoplanktonic C and microbial net production, was observed at station E178. At station E168, vertical flux percentages were 4.5 times lower in relation to suspended phytoplankton biomass, and 3.5 times lower with respect to primary production rate. At station E184, dominated by phytoplankton >10 μm and with the highest total sedimentation rate, both percentages were, however, relatively low and very similar to those obtained in Bransfield.

Table I: Vertical fluxes of particulate material (± SE, n = 4) collected by sediment traps. The percentage corresponding to phytoplankton-derived material with respect to total particulate organic carbon, assuming a C/chlorophyll a ratio of 40, is presented. C incorporation by phytoplankton collected in the traps and incubated under light saturating conditions is also given

Station	Carbon (mg m^{-2} day^{-1})	Chlorophyll *a* (mg m^{-2} day^{-1})	%C (Chl *a*)	C incorporation (mgC m^{-3} h^{-1})	Faecal pellets (no. m^{-2} day^{-1} × 10^5)
E168	115 ± 30	0.73 ± 0.02	25	1.37 ± 0.13	0
E178	237 ± 36	0.79 ± 0.03	13	1.24 ± 0.04	2.3 ± 1.7
E184	470 ± 28	12.72 ± 0.86	108	1.11 ± 0.18	12.6 ± 2.5

Phytoplankton growth and loss rates

Specific phytoplankton growth rate was calculated as ln[(biomass+GP)/biomass]/ln(2) from GP data, converted to carbon using a photosynthetic quotient of 1.4, which assumes that GP was based on nitrate (Laws, 1991), and from chlorophyll *a* data, assuming a carbon to chlorophyll *a* ratio of 40 (Smith and Sakshaug, 1990). The specific loss rate of phytoplankton biomass through sinking was estimated from the daily rate of carbon sedimentation, calculated from the sediment traps, and from integrated chlorophyll *a* concentration. The loss rate through zooplankton grazing was estimated from the respiration rate of mesozooplankton, calculated from integrated (0–200 m) zooplankton biomass in three size classes (200–500 μm, 500–1000 μm and >1000 μm) (Cabal *et al.*, 2002), by means of the allometric relation of body length to fresh weight in planktonic crustaceans (Peters, 1983), and the relation of mesozooplankton respiration to individual weight and temperature [(Ikeda, 1985), as shown in (Zhang *et al.*, 1995)]. Carbon demand by mesozooplankton was calculated assuming an assimilation efficiency of 70% (Conover, 1978). Grazing rate by microzooplankton is already included in the total loss rate through microbial respiration, which represents its highest limit. Assuming that steady state and exponential growth prevailed during the period between the sampling of the transect and the flux stations, total phytoplankton biomass loss rate (ΔChl *a*-derived loss rate) was calculated, from the difference between the local rate of change in phytoplankton biomass and the growth rate calculated from primary production and phytoplankton biomass. The results of these calculations are shown in Table III. The highest growth and loss rates (both by sedimentation and grazing) were measured at the frontal station (E178). At stations E184 (Gerlache) and E168 (Bransfield) similar rates were obtained, except for microbial respiration, which was twice as high at E184. Very low growth rates were measured at station E169 (Gerlache), where grazing losses were also very low. Only at station E178 did the sum of loss rates by sedimentation

Table II: Water column (0–50 m) integrated values of suspended phytoplankton carbon (Csusp. Calculated from chlorophyll-a concentration and a C/Chl a ratio of 40), photosynthetic C incorporation (Cinc), microbial net production (NCP; converted to g C m^{-2} day^{-1} assuming a molar ratio of net oxygen production to carbon incorporation of 1.5), vertical flux of carbon (VF). %Csusp, %Cinc and %NCP represent, respectively, the percentages of VF with respect to Csusp, Cinc and NCP in the water column above the sediment trap

Station	Csusp (gC m^{-2})	Cinc (gC m^{-2} day^{-1})	NCP (gC m^{-2} day^{-1})	VF (mgC m^{-2} day^{-1})	%Csusp	%Cinc	%NCP
E169	18.6	1.1	0.8				
E184	7.4	3.0	3.2	470	6.4	15.5	14.9
E178	1.1	0.5	0.7	237	21.9	48.4	35.3
E168	2.2	0.8	1.1	115	5.1	14.5	10.4

Table III: Phytoplankton biomass specific growth rate and loss rates (day^{-1}) by sedimentation, mesozooplankton grazing and microbial respiration in the mixed layer at flux stations. ∑ S losses represents the sum of the above specific loss rates. ΔChl a S loss represent the phytoplankton biomass loss rate calculated from the change in chlorophyll a concentration in the upper mixed layer between sampling of the transect and the flux stations. Percentage of phytoplankton >10 μm is presented, both as biomass and production (±SE), for reference

	E184	E169	E178	E168
Phytoplankton >10 μm				
Chlorophyll a (%)	78.1±4.7	86.4±4.6	24.3±4.2	8.6±1.0
Carbon incorporation (%)	48.2±13.1	64.0±12.4	11.0±0.9	9.5±1.4
S growth	0.66	0.12	1.11	0.69
S sedimentation	0.088	n.d.	0.286	0.072
S mesozooplankton grazing	0.003	0.001	0.013	0.004
S microbial respiration	0.30	0.08	0.85	0.15
∑ S losses	0.39		1.14	0.23
ΔChl *a* S loss	0.70		1.17	0.73

and grazing amount to a value similar to the ΔChl *a*-derived loss rate. At stations E184 and E168 the latter was greater than the sum of the former.

DISCUSSION

Most conceptual models on plankton dynamics predict low DR in relation to GP (i.e. elevated NCP), as well as a high percentage of sedimentation in relation to suspended material and/or primary production, for large-sized phytoplankton communities, such as those found in Gerlache Strait. In the pico- and nanoplankton-dominated communties of Bransfield, however, a higher percentage of gross production would be expected to be respired within the mixed layer, while vertical particle flux and chlorophyll *a* content in the sedimented material should be lower.

As expected, the highest contribution of phytoplankton to total sedimentation rate was registered at the station located at the centre of the Gerlache diatom bloom (E184). Mesozooplankton activity appeared to influence strongly the vertical transport, as reflected by the high number of faecal pellets, and the low specific activity of the sedimented phytoplanktonic material (Table I).

However, and against theoretical predictions, the lowest DR rates were measured at the pico- and nanoplankton-dominated station of Bransfield (E168) and the highest at E184. Moreover, negative values of NCP were only measured in Gerlache, below the euphotic zone (Figure 8), in agreement with the higher activity of bacteria and protist measured in Gerlache than in Bransfield during this study (Pedrós-Alió *et al.* 2002; Vaqué *et al.*, 2002) and with the gradient in respiration observed by Arístegui and Montero (Arístegui and Montero, 1995) over the same area. In addition, the highest relative rate of vertical particle flux, both with respect to suspended phytoplanktonic C and integrated NCP, was found at the frontal station E178, dominated by *Cryptomonas* sp., and no difference in the percentage of sedimentation was observed between stations E184 (diatom maximum) and E168 (nanoplankton), despite the large differences in community structure, total phytoplankton biomass and primary production.

To explore the reasons for these unexpected results and, in general, to understand the influence of diverse factors (specifically, community structure) on the relationship between production and export of organic carbon, it is important to appreciate the growth conditions of the community, as those relationships may be different in systems that are transient or close to equilibrium. In the case of those flux stations where little variation occurred in both the physical and biological fields between the sampling of the transect and flux stations, steady state may be presumed for that period of time. Then, the local rate of change in phytoplankton biomass is given by the expression: dF/dt = growth – advection + diffusion – sedimentation – consumption (Frost, 1991). On this basis, an analysis of phytoplankton growth and loss processes has been performed for each community in order to (1) ascertain the origin of observed local biomasses, (2) verify whether the processes of production and export of

organic matter were acting at coupled spatial and temporal scales, and (3) determine the processes responsible for the observed disagreement with theoretical predictions.

Communities dominated by large-sized (>10 μm) phytoplankton

Physical conditions in the water column, phytoplankton size spectrum, floristic composition and spatial distribution of phytoplankton biomass and production remained almost unaltered in the central region of Gerlache between the two sampling times.

Estimated phytoplankton growth rate was very high (0.66 day^{-1}) at the centre of this patch (E184). Assuming that such a growth rate remained constant throughout the 12 days of study, the ΔChl *a*-derived phytoplankton biomass loss rate is estimated as 0.7 day^{-1} (Table III), much higher than the sum of loss rates through sinking and grazing (0.39 day^{-1}), which implies that either the balance between advection and diffusion was responsible for a loss of phytoplanktonic biomass of 0.3 day^{-1}, and/or that the calculated loss rate by zooplankton grazing, obtained from zooplankton biomass, underestimates the actual value. Calculated zooplankton respiration rates are coherent with rates experimentally obtained for *Metridia gerlachei* during FRUELA96 cruise [4.17 μl O_2 mg C^{-1} h^{-1}. (Calbet and Irigoien, 1997)], as well as with the literature (Martens, 1992). A similar impact of Antarctic zooplankton on phytoplanktonic biomass has frequently been observed (Mitchell and Holm-Hansen, 1991; Atkinson and Shreeve, 1995), and seems reasonable for early spring, considering the uncoupling in zooplankton and phytoplankton growth. Nevertheless, it is still possible that zooplankton biomass obtained from vertical tows will not properly represent total potential grazing pressure, due to the aggregated distribution and high mobility of krill. However, the permanence of an almost absolute dominance of cells >10 μm during the period of study in Gerlache Strait, would suggest a non-significant impact of krill (Lancelot *et al.*, 1993).

At the margin of the high chlorophyll *a* patch of Gerlache (E169), vertical stability conditions changed in the 5 days separating both samplings (Figure 4). This fact, and the boundary position of this station, made the calculation of ΔChl *a*-derived loss rate impossible. Nevertheless, the similar phytoplankton size spectra at stations E184 and E169, and the much lower growth rate at the latter, suggest that total losses at E169 would be similar to, if not greater than, those at E184, as shown by the vertical patterns of respiration (Figure 9), which suggest that sinking rate was greater at E169.

Phytoplankton growth rate at E169 was very low (0.12 day^{-1}), certainly not able to explain the observed biomass in the mixed layer. With such a growth rate, a loss rate similar to that calculated for station E184 would have caused a decrease in chlorophyll *a* concentration to values near 0.5 mg m^{-3} in 5 days. Even with a lower loss rate, considered normal in this region [0.2–0.3 day^{-1}, (Mitchell and Holm-Hansen, 1991); 0.05–0.3 day^{-1}, (Lancelot *et al.*, 1993); 0.2–0.32 day^{-1}, (Boyd *et al.*, 1995) in Bellingshausen Sea], *in situ* growth at E169 would not suffice to maintain the observed biomass. Hence, part of this biomass at station E169 might derive from adjacent regions. Such a deficit is consistent with expectations from most Antarctic phytoplankton growth models (Mitchell and Holm-Hansen, 1991; Nelson and Smith, 1991; Sakshaug *et al.*, 1991; Svansson, 1991; Lancelot *et al.*, 1993), which conclude that, when nutrients are not limiting, a total loss rate of 0.3–0.35 day^{-1} requires a mixed layer not deeper than 25–30 m to allow the development of phytoplankton blooms (see Figure 4). In the present study, as observed previously (Mitchell and Holm-Hansen, 1991) for the same region during December to March, a chlorophyll *a* concentration higher than 10 mg m^{-2} only persisted in areas with upper mixed layer depths of 20 m (see Figures 2 to 5). Such a shallow mixed layer depth for bloom development, as well as observed changes in chlorophyll *a* concentration at both E184 and E169, together with the low microbial respiration rates, suggest the greater relative importance of other loss processes in the control of phytoplankton populations in the central region of Gerlache Strait. These losses, specifically the balance between diffusion and advection, would account for the surplus of production at the centre of the high biomass patch and would cause the marginal region to be dependent upon organic matter import.

Communities dominated by nanoplankton (2–10 μm) under vertical stability conditions

The highest phytoplankton growth rates for the whole region of study were measured at the frontal station (E178), in the Gerlache–Bransfield confluence. The high biomass of small phytoplankton remained after 10 days (Figures 3 and 5), thus allowing the calculation of ΔChl *a*-derived loss rate. Such a high loss rate (1.17 day^{-1}) was only compensated by phytoplankton growth at the surface (1.41 day^{-1}), where most of phytoplankton biomass and production, and microbial respiration were confined.

Under situations of stability and dominance of nanoplankton, such as those observed at E178, coupling between production and consumption usually occur (Riegman *et al.*, 1993; Legendre and Rassoulzadegan, 1996). As expected, the highest specific loss rate due to microbial respiration was registered at station E178 (Table III). The comparison between stations E178 and E168, both dominated by *Cryptomonas* sp., indicate that

microheterotrophic consumption at station E178 (where small dinoflagellates were also abundant) was very important. If the contribution of phytoplanktonic respiration to total consumption of oxygen is estimated, assuming this value to be 12% of gross production (Setchell and Packard, 1979), it would represent 98% of total respiration at station E168 (0–50 m) and only 25% at station E178.

Although the ΔChl *a*-derived loss rate at E178 (1.17 day^{-1}) was very similar to the sum of loss rates by grazing and sedimentation (1.14 day^{-1}), the measured sedimentation rate (0.29 day^{-1}) was more than three times higher than the highest values found in the literature for polar regions [0.005–0.07 day^{-1}; (von Bodungen *et al.*, 1986; Wassman *et al.*, 1990; Mitchell and Holm-Hansen, 1991; Karl *et al.*, 1991). Such a high value, however, can only explain the observed decrease in mixed layer chlorophyll *a* concentration of 1.5 mg m^{-3} in 10 days. It is clear that the convergent front located at this zone not only gives rise to conditions favouring phytoplankton accumulation and growth, but also provides a mechanism for sinking of organic carbon, as shown in the spatial distributions of phytoplankton biomass (Figure 3) and microbial activity (Figure 8). Moreover, the carbon incorporation rate by material collected with the sediment trap was very high in relation to chlorophyll *a* content, which also suggests rapid sinking of phytoplankton cells.

Communities dominated by nanoplankton (2–10 μm) under vertical mixing conditions

Phytoplankton size distribution, abundance of dominant taxa, and total chlorophyll *a* concentration in the mixed layer (1.59–1.45 mg m^{-3}) remained almost unchanged during the 3 days separating both samplings of station E168 (Bransfield). Phytoplankton-specific growth rate was very high (1.01 day^{-1} at the surface, 0.69 day^{-1} in the mixed layer) and the ΔChl *a*-derived loss rate gave a critical depth >120 m. These very high values do not agree with the low chlorophyll *a* concentration (62 mg m^{-2}) observed in a mixed layer of 40 m, especially considering the even distribution of phytoplankton biomass and production in this layer (see Figures 4 and 9), not linked to the pycnocline.

In Bransfield, the molar ratio of net oxygen production to carbon incorporation in the photic layer was >2, suggesting a significant production of dissolved organic matter (DOM) by phytoplankton. This conclusion is in agreement with the high values of DOC production (23% of total carbon incorporation) measured by Morán and Estrada (Morán and Estrada, 2002) in Bransfield Strait. The very low heterotrophic activity measured in this region might produce the accumulation of DOM and, as suggested previously for the same region (Karl *et al.*, 1991), its possible exportation.

ΔChl *a*-derived loss rate (even from C incorporation) was higher than the sum of loss rates by sedimentation and grazing (Table III). Specific loss rate by sedimentation was relatively high (Karl *et al.*, 1991), and microheterotrophic consumption was necessarily less than total microbial respiration, hence such a disagreement must derive from either an underestimate of mesozooplankton and krill impact, or a negative balance between advection and diffusion.

The very low DR rates measured at station E168 and reduced microheterotrophic contribution to total respiration (ca. 2% of total respiration, 0–50 m) suggest that the mechanism regulating phytoplankton biomass and, especially, size structure, might be related to the control of microzooplankton grazing rather than to light or nutrient limitation of large phytoplankton growth. Minimum values were found for both large protist biomass and consumption of bacterial biomass by protists in Bransfield waters (Vaqué *et al.*, 2002). Chlorophyll *a*-normalized C incorporation rates of phytoplankton >10 μm were very high at this station (>70 mg C mg Chl a^{-1} day^{-1}). Moreover, the contribution of phytoplankton-derived material to the vertical flux of particles was considerably higher than at the other nanoplankton-dominated station, and activity of sedimented phytoplankton was high, despite no clear hydrodynamic mechanism leading to the rapid sinking of material. Although it can be argued that a decrease in microzooplankton activity should have been reflected in an increase in bacterial numbers, the results indicate that bacterial abundance and activity in the region were not controlled by bacterivory due to protists (Vaqué *et al.*, 2002), but by temperature and predation by viruses (Guixa-Boixereu *et al.*, 2002; Pedrós-Alió *et al.*, 2002).

Conclusions: trophic control of biogenic carbon export

The results obtained in this investigation failed to show a direct relationship between phytoplankton size or P/R balance and biogenic carbon export. A similar result lead Rivkin *et al.* (Rivkin *et al.*, 1996) to conclude that food web structure cannot be used to predict the magnitude or patterns of biogenic carbon export from the ocean surface. In our opinion, however, these negative results imply that the relationship between food web structure and biogenic carbon export is far more complex than considered by conceptual models on the trophic control of C export (Legendre and Rassoulzadegan, 1996). These models rely on the existence of a functional link between population and trophic dynamics, and assume that the trophic functioning of a planktonic community may be ascertained from its current structure, usually defined from phytoplankton size. The consideration of DOM as a dynamic

constituent of pelagic food webs implies that such an assumption may not always be valid. Accumulation of DOM as a consequence of a concurrent limitation of microbial consumption [(Hansell and Carlson, 1998; Fasham *et al.*, 1999) and references therein] does not provide any information on the final fate of organic matter produced in the euphotic zone, but simply indicates that the scale of ecosystem functioning may be longer than usually considered. In addition to direct export of the DOC excess, its accumulation in the upper mixed layer may give rise to the linkage of production and consumption of organic matter over large spatial or long temporal scales (Pomeroy and Wiebe, 1993; Sherr and Sherr, 1996), thus allowing the metabolic compensation of otherwise separated communities, hence affecting food web structure and the trophic balance at local scales (Serret *et al.*, 1999). Consequently, although the downward POC flux will be dependent on the concurrent phytoplankton size (Boyd and Newton, 1999), the estimation of the ecosystem export potential from the latter may be uncertain. A seasonal uncoupling between phytoplankton and bacterioplankton activities has been observed in Antarctic waters (Delille and Mallard, 1991) suggesting the possibility of a long-term linkage of production and respiration of organic matter. Such a process characterizes the seasonal dynamics of some coastal temperate planktonic ecosystems (Serret *et al.*, 1999) and could underlie the concurrent observation of net heterotrophy and biogenic carbon export in postbloom conditions (Rivkin *et al.*, 1996). The uncoupling of production and respiration would in turn broaden the role played by hydrodynamics in C export control. Hydrodynamics would not only regulate phytoplankton size spectra and activity (Kiørboe, 1993), and the immediate linkage between producers and heterotrophs (Legendre and Rassoulzadegan, 1996), but would also be a mechanism producing a short-circuit in the long-term linkage between production and oxidation of DOM.

The present investigation emphasizes the importance of precisely determining the processes and of re-examining the scales of organic matter circulation in planktonic ecosystems, and points out the limitations inherent to studies of trophic control of carbon export (Rivkin *et al.*, 1996) conducted over scales shorter than those of linkage between production and respiration of organic matter in the sea.

ACKNOWLEDGEMENTS

This study was undertaken as part of CICYT's ANT 95/1195 project. P. Serret was supported by a PFPI grant from the Spanish Ministerio de Educación y Ciencia and a grant from the Universidad de Oviedo within the European Commission project CE-96-MAS3-CT-0060. This paper was written while P. Serret was funded by an EU TMR Marie Curie Research Training Grant (ERBFMBICT972700). We appreciate the work at sea of the crew of BIO Hespérides. We are much indebted to M. Quevedo, I. Huskin, R. González-Quirós, J. L. Acuña, J. Cabal, M. Alcaraz and R. Martínez for their help with calculations of mesozooplankton respiratory activity, to C. Robinson for her support during the writing of the manuscript and to C. Fernández for her assistance with the figures.

REFERENCES

Arístegui, J. and Montero, M. F. (1995) Plankton community respiration in Bransfield Strait (Antarctic Ocean) during austral spring. *J. Plankton Res.*, **17**, 27–39.

Atkinson, A. and Shreeve, R. S. (1995) Response of the copepod community to a spring bloom in the Belligshausen Sea. *Deep-Sea Res. II*, **42**, 1291–1311.

Biscaye, P. E., Flagg, C. N. and Falkowski, P. G. (1994) The Shelf Edge Exchange Processes experiment, SEEP-II: an introduction to hypotheses, results and conclusions. *Deep-Sea Res. II*, **41**, 231–252.

Boyd, P., Robinson, C., Savidge, G. and Williams, P. J. le B. (1995) Water column and sea-ice primary production during Austral spring in the Bellingshausen Sea. *Deep-Sea Res. II*, **42**, 1177–1200.

Boyd, P. W. and Newton, P. P. (1999) Does planktonic community structure determine downward particulate organic carbon flux in different oceanic provinces? *Deep-Sea Res. I*, **46**, 63–91.

Buesseler, K. O. (1998) The decoupling of production and particulate export in the surface ocean. *Global Biogeochem. Cycles*, **12**, 297–310.

Cabal, J. A., Álvarez-Marqués, F., Acuña, J. L., Quevedo, M., G.-Quirós, R., Huskin, I., Fernández, D., Rodriguez del Valle, C. and Anadón, R. (2002) Mesozooplankton distribution and grazing during the productive season in the Northwest Antarctic Península (FRUELA cruises). *Deep-Sea Res. II* (in press).

Calbet, A. and Irigoien, X. (1997) Egg and fecal pellet production rates of the marine copepod Metridia gerlachei in the NW of the Antarctic Peninsula. *Polar Biol.*, **18**, 273–279.

Castro, C. G., Rios, A. F., Doval, M. D. and Perez, F. F. (2002) Spatio-temporal variability of nutrient utilisation and chlorophyll distribution in the upper mixed layer during FRUELA95 and FRUELA96 cruises (Antarctica). *Deep-Sea Res. II* (in press).

Conover, R. J. (1978) Transformation of organic matter. In Kinne, O. (ed.), *Marine Ecology*. Wiley, London, Vol. 4, pp. 221–499.

Delille, D. and Mallard, L. (1991) Seasonal changes of Antarctic marine bacterioplankton. *Kieler Meeresforschungen, Sonderheft*, **8**, 213–218.

Fasham, M. J. R., Boyd, P. W. and Savidge, G. (1999) Modelling the relative contribution of autotrophs and heterotrophs to carbon flow at a Lagrangian JGOFS station in the Northeast Atlantic: The importance of DOC. *Limnol. Oceanogr.*, **44**, 80–94.

Frost, B. W. (1991) The role of grazing in nutrient-rich areas of the open ocean. *Limnol. Oceanogr.*, **36**, 1616–1630.

Grasshoff, K., Ehrhardt, M. and Kremling, M. (1983) *Methods of Seawater Analysis*, 2nd edn. Verlag Chemie, Weinheim.

Guixa-Bioxereu, N., Vaqué, D., Gasol, J. M., Sánchez-Cámara, J. and Pedrós-Alió, C. (2002) Viral distribution and activity in Antarctic waters. *Deep-Sea Res. II*, (in press).

Hansell, D. A. and Carlson, C. A. (1998) Net community production of dissolved organic carbon. *Global Biogeochem. Cycles*, **12**, 443–453.

Holm-Hansen, O. and Mitchell, B. G. (1991) Spatial and temporal distribution of phytoplankton and primary production in the western Bransfield Strait region. *Deep-Sea Res.*, **38**, 961–980.

Ikeda, T. (1985) Metabolic rates of epipelagic marine zooplankton as a function of body size and temperature. *Mar. Biol.*, **104**, 1–11.

Karl, D. M. (1993) Microbial processes in the Southern Ocean. In Friedman, E. I. (ed.), *Antarctic Microbiology*. John Wiley and Sons, New York, pp. 1–63.

Karl, D. M., Tilbrook, B. D. and Tien, G. (1991) Seasonal coupling of organic matter production and particulate flux in the western Bransfield Strait, Antarctica. *Deep-Sea Res.*, **38**, 1097–1126.

Kiørboe, T. (1993) Turbulence, phytoplankton cell size, and the structure of pelagic food webs. *Adv. Mar. Biol.*, **29**, 1–72.

Knap, A., Michaels, A., Close, A., Ducklow, H. and Dickson, A. (eds) (1996) Protocols for the Joint Global Ocean Flux Study (JGOFS) Core Measurements. JGOFS Report Nr. 19, vi+170 pp. Reprint of the IOC Manuals and Guides No. 29, UNESCO1994. 155–162.

Knauer, G. A., Martin, J. H. and Bruland, K. W. (1979) Fluxes of particulate carbon, nitrogen and phosphorus in the upper water column of the northeast Pacific. *Deep-Sea Res.*, **26**, 97–108.

Lancelot, C., Mathot, S., Veth, C. and de Baar, H. (1993) Factors controlling phytoplankton ice-edge blooms in the marginal ice-zone of the northwestern Weddell Sea during sea ice retreat 1988: field observations and mathematical modelling. *Polar Biol.*, **13**, 377–387.

Laws, E. A. (1991) Photosynthetic quotients, new production and net community production in the open ocean. *Deep-Sea Res.*, **38**, 143–167.

Legendre, L. and Le Fèvre, J. (1989) Hydrodynamical singularities as controls of recycled versus export production in oceans. In Berger, W. H., Smetaceck, V. S. and Wefer, G. (eds), *Productivity of the Oceans: Present and Past*. John Wiley & Sons, Chichester, pp. 44–63.

Legendre, L. and Rassoulzadegan, F. (1995) Plankton and nutrient dynamics in marine waters. *Ophelia*, **41**, 153–172.

Legendre, L. and Rassoulzadegan, F. (1996) Food-web mediated export of biogenic carbon in oceans: hydrodynamic control. *Mar. Ecol. Prog. Ser.*, **145**, 179–193.

Lignell, R., Heiskanen, A. S., Kuosa, H., Gundersen, K., Kuuppo-Leinikki, P., Pajuniemi, R. and Uitto, A. (1993) Fate of a phytoplankton spring bloom: sedimentation and carbon flow in the planktonic food web in the northern Baltic. *Mar. Ecol. Prog. Ser.*, **94**, 239–252.

Martens, P. (1992) Zooplankton community respiration during the JGOFS pilot study. *Helgoländer Meeresunters*, **46**, 117–135.

Mitchel, B. G. and Holm-Hansen, O. (1991) Observations and modelling of the Antarctic phytoplankton crop in relation to mixing depth. *Deep-Sea Res.*, **38**, 981–1007.

Moline, M. A. and Prézelin, B. B. (1996) Long-term monitoring and analyses of physical factors regulating variability in coastal Antarctic phytoplankton biomass, *in situ* productivity and taxonomic composition over subseasonal, seasonal and interannual time scales. *Mar. Ecol. Prog. Ser.*, **145**, 143–160.

Morán, X. G. and Estrada, M. (2002) Phytoplankton DOC and POC production in the Bransfield and Gerlache Straits as derived from kinetic experiments of 14C incorporation. *Deep-Sea Res. II*, (in press).

Nelson, D. M. and Smith Jr., W. O. (1991) Sverdrup revisited: Critical depths, maximum chlorophyll levels, and the control of Southern Ocean productivity by the irradiance-mixing regime. *Limnol. Oceanogr.*, **36**, 1650–1661.

Newton, P. P., Lampitt, R. S., Jickells, T. D., King, P. and Boutle, C. (1994) Temporal and spatial variability of biogenic particles fluxes during JGOFS northeast Atlantic process studies at 47°N, 20°W. *Deep-Sea Res I*, **41**, 1617–1642.

Oudot, C., Gerard, R., Morin, P. and Gningue, I. (1988) Precise shipboard determination of dissolved oxygen (Winkler procedure) for productivity studies with a commercial system. *Limnol. Oceanogr.*, **33**, 146–150.

Pedrós-Alió, C., Vaqué, D., Guixa-Boixereu, N. and Gasol, J. M. (2002) Prokaryotic plankton biomass and heterotrophic production in western Antarctic waters, during the 1995–96 austral summer. *Deep-Sea Res. II*, (in press).

Peters, R. H. (1983) *The Ecological Implications of Body Size*. Cambridge University Press, Cambridge.

Pomeroy, L. R., Sheldon, J. E. and Sheldon Jr., W. M. (1994) Changes in bacterial numbers and leucine assimilation during estimations of microbial respiratory rates in seawater by the precision Winkler method. *Appl. Environ. Microb.*, **60**, 328–332.

Pomeroy, L. R. and Wiebe, W. J. (1993) Energy sources for microbial food webs. *Mar. Microb. Food Webs*, **7**, 101–118.

Riegman, R., Kuipers, B. R., Noordeloos, A. A. M. and Witte, H. (1993) Size-differential control of phytoplankton and the structure of plankton communities. *Neth. J. Sea. Res.*, **31**, 255–265.

Rivkin, R. B., Legendre, L., Deibel, D., Tremblay, J. E., Klein, B., Crocker, K., Roy, S., Silverberg, N., Lovejoy, C., Mesplé, F., Romero, N., Anderson, M. R., Matthews, P., Savenkoff, C., Vézina, A., Therriault, J. C., Wesson, J., Bérubé, C. and Ingram, G. (1996) Vertical flux of biogenic carbon in the ocean: is there food web control? *Science*, **272**, 1163–1166.

Sakshaug, E., Slagstad, D. and Holm-Hansen, O. (1991) Factors controlling the development of phytoplankton blooms in the Antarctic Ocean – a mathematical model. *Mar. Chem.*, **35**, 259–271.

Serret, P., Fernández, E., Álvarez-Sostres, J. and Anadón, R. (1999) Seasonal compensation of microbial production and respiration in a temperate sea. *Mar. Ecol. Prog. Ser.*, **187**, 43–57.

Setchell, F. W. and Packard, T. T. (1979) Phytoplankton respiration in the Peru Upwelling. *J. Plankton Res.*, **1**, 343–354.

Sherr, E. B. and Sherr, B. F. (1996) Temporal offset in oceanic production and respiration processes implied by seasonal changes in atmospheric oxygen: the role of heterotrophic microbes. *Aquat. Microb. Ecol.*, **11**, 91–100.

Smith, W. O. and Sakshaug, E. (1990) Polar phytoplankton. In: Smith, W. O. Jr (ed.) *Polar Oceanography, Part B: Chemistry, Biology and Geology*. Academic Press, Inc., San Diego, pp. 477–525.

Strickland, J. D. H. and Parsons, T. R. (1972) *A Practical Handbook of Seawater Analysis*, 2nd edn. Fisheries Research Board of Canada, Ottawa.

Svansson, A. (1991) A simple primary production model for the NW Weddell Sea. *Mar. Chem.*, **35**, 347–354.

Vaqué, D., Guixa-Bioxereu, N., Gasol, J. M. and Pedrós-Alió, C. (2002) Distribution of microbial biomass and importance of protist in regulating prokaryotic assemblages in three areas close to the Antarctic Península in Spring and summer 1995/96. *Deep-Sea Res. II*, (in press).

von Bodungen, B., Smetacek, V., Tilzer, M. M. and Zeitzschell, B. (1986)

Primary production and sedimentation during spring in the Antarctic Peninsula region. *Deep-Sea Res.*, **33**, 177–194.

Wassman, P., Vernet, M. and Mitchell, B. G. (1990) Mass sedimentation of *Phaeocystis* pouchetii in the Barents Sea. *Mar. Ecol. Prog. Ser.*, **66**, 183–195.

Williams, P. J. le B. and Robertson, J. E. (1991) Overall planktonic oxygen and carbon dioxide metabolisms: the problem of reconciling observations and calculations of photosynthetic quotients. *J. Plankton Res.*, **13** (supplement):153–169.

Zhang, X., Dam, H. G., White, J. R. and Roman, M. R. (1995) Latitudinal variations in mesozooplankton grazing and metabolism in the central tropical Pacific during the US JGOFS EqPac study. *Deep-Sea Res. II*, **42**, 695–714.

Received on May 13, 2000; accepted on July 5, 2001